*2012 International Conference on Fluid Dynamics and Thermodynamics Technologies (FDTT 2012)*
***IPCSIT vol.33(2012)©(2012) IACSIT Press, Singapore***

# Numerical investigation of drag reduction in microchannels with superhydrophobic walls consist of aligned and staggered microposts

Masoud Kharati Koopaee[1 +],Mohsen Jahanmiri[1], Hosein Mahmood Zadeh[1]
1 Department of Aerospace and Mechanical Eng., Shiraz University of Technology, Shiraz, Iran

**Abstract**. In this research, based on the numerical simulation, drag reduction in laminar flow in microchannels with superhydrophobic walls comprised of aligned and staggered microposts for different values of relative modules width, cavity fractions and Reynolds number are presented. Grid independency study is also carried out to ensure grid independent results. Results show that the friction factor-Reynolds number product for aligned posts is less than that of staggered one. The deviation between two configurations was found to be higher for increasing values of relative module width. Further, numerical results show that increasing Reynolds number would lead to higher difference in friction factor-Reynolds number product between these two configurations. It is also found that the non-dimensional slip length for aligned microposts is higher than that of staggered arrangement.

**Keywords:** drag reduction, microchannel, microposts, laminar flow, superhydrophobic

## 1. Introduction

One of the most important passive techniques for drag reduction in microchannel is to use the superhydrophobic surfaces. In these surfaces, the hydrophobicity along with the micro or nano-scale roughness would lead to an effect that is known as superhydrophobicity. The most significant feature of the superhydrophobicity is to provide the contact angle more than $150$ degrees for a water droplet placed on such surfaces.

The common shapes of a superhydrophobic surface are ribs and cavities that may be oriented parallel or transverse to the main stream. The other shape may be a combination of posts and cavities in aligned or staggered form. Constructing a square by four posts, the main flow direction is parallel to a side of square in the aligned configuration while in the staggered form, the main stream is parallel to the diagonal of the square. Recently, the superhydrophobic surface comprised of random roughness has also received attention by some researchers [1]. Since the cavities are in micro or nano-scales, they prevent penetration of liquid into the cavities. Nearly a free shear area exists in the superhydrophobic surface at the interface of fluid and cavity. Thus, lower drag appears in such channels in comparison with those have solid surfaces as channel walls.

Many studies are performed on the superhydrophobic surfaces. These studies include the theoretical, numerical and experimental approaches. Philip [2,3] studied the flow over superhydrophobic surfaces theoretically. His work is viewed as the first theoretical work on such surfaces. Other researchers [4,5] also had a theoretical approach and solved the stokes flow over such surfaces. Some researchers used the numerical approaches for flow simulations over theses surfaces [6-12]. These approaches use the finite element, finite volume, lattice Boltzmann or direct numerical simulation (DNS) methods to simulate the flow over superhydrophobic surfaces. In these studies, both laminar and turbulent flows over microposts, random roughness or microridge configurations in parallel or transverse to the flow direction were concerned. For instance, Hirsa [10] investigated the effective slip length of transverse grooves, longitudinal grooves, posts and holes in laminar flow. Martell et al. [11] used DNS solution of flow over micropost and microridge arrangements and showed that in turbulent flows the drag reduction is increased as an increase exists in the flow rate and Reynolds number. Jeffs et al. [12] demonstrated that reduction in friction factor was greater for turbulent flow than for laminar flow under the same geometric condition. Other works on the superhydrophobic surfaces found in the literature are associated with the experimental approaches [13-15].

+ Corresponding author. Tel.: +987117264102; fax: +987117264102
E-mail address: kharati@sutech.ac.ir

The techniques used in these works were generally particle image velocimetry (PIV) and pressure drop measurements.

As can be seen in the literature, the pervious works are concerned with numerical or experimental approach on the understanding of behavior of superhydrophobic surfaces consists of microridges or microposts. Some works are also involved in comparative study between microridge and microposts arrangements. However, no researches could be found on the drag reduction study of different pattern (i.e. aligned and staggered) of microposts superhydrophobic surfaces. In this research, the drag reduction effect in microchannels with superhydrophobic surfaces comprised of different patterns of microposts is of interest and the effects of relative module width, cavity fractions and Reynolds number on the friction factor-Reynolds number product and slip length are investigated.

## 2. Methodology and Problem Definition

In present study, a fully developed incompressible laminar flow is assumed. So, the Navier-Stokes equations with constant density and viscosity are solved on the fluid domain with a finite volume based code. In this work, the flow through an infinite width rectangular microchannel with two different patterns of superhydrophobic walls consists of microposts in aligned and staggered forms are considered. The superhydrophobic surfaces used as the top and bottom of the microchannel walls. Fig. 1 depicts the two mentioned different patterns and direction of flowing fluid. Dark regions represent the computational domain.

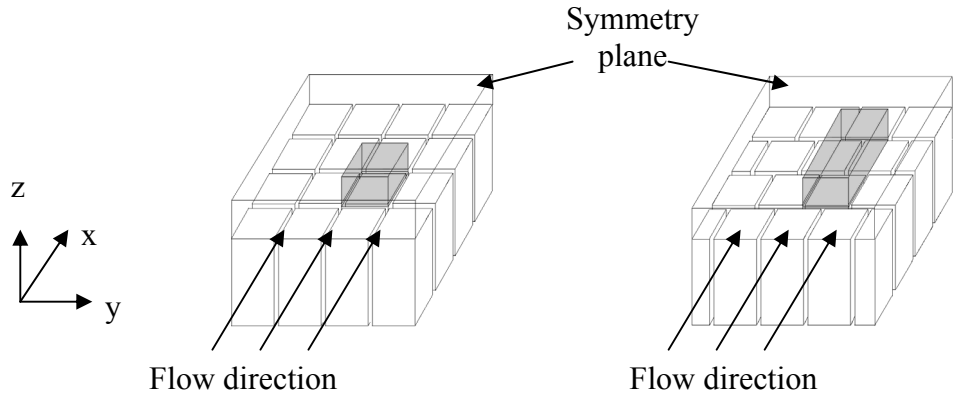


Fig. 1: The aligned (left) and staggered (right) microposts used as the microchannel walls.

Fig. 2 presents these two arrangements viewed from the top. The dashed lines show the computational domain used for numerical analysis. In this figure, $W$ represents combined post and cavity width and $W_c$ is the cavity width.

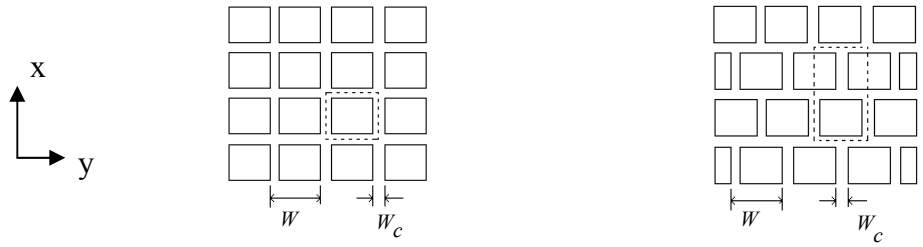


Fig. 2: Two different patterns of superhydrophobic surface viewed from the top.

The Reynolds number is defined based on the microchannel hydraulic diameter, $Re = \rho\, u_m\, D_h / \mu$. In this definition, $\rho$, $u_m$ and $D_h$ are density, mean velocity and hydraulic diameter and $\mu$ is liquid viscosity. The hydraulic diameter is also based on the liquid area and total liquid perimeter, $D_h = 4\, A / P_w$, where $A$ is the flow area and $P_w$ is the liquid perimeter. The flow area is $A = 2\, h\, b$, where $h$ is half of the distance between top and bottom walls and $b$ is the channel width. In the case of the infinite width microchannel where $b \to \infty$, the hydraulic diameter would be $D_h = 4\, h$. Here, the relative module width is

$W_m = W / D_h$, where $W$ is the combined post and cavity width. The cavity fraction is also defined as $F_c = A_f / A_t$, where $A_f$ and $A_t$ are the free shear and total areas, respectively.

## 3. Grid Independency Study

As mentioned earlier, all numerical results are obtained utilizing a finite volume based code. The interface between water and air is considered as a flat free shear surface. As presented in [16], the free shear assumption between water-air interface is a good approximation when gas-liquid viscosity ratio is about $10^{-2}$ or less. The interface between fluid and wall would also be a no slip surface. Owing to the symmetry, half of the microchannel height is considered for analysis. As shown in Fig. 1, the bottom of the control volume used for numerical analysis includes the free shear and no slip conditions, while the top is considered as a symmetry plane. The other four sides of the control volume are modeled as periodic surfaces. In the current study, the Reynolds number is varied from $100$ to $2000$ and relative module width is varied from $0.1$ to $0.9$ and cavity fraction range of $0.1$ to $0.97$ is considered.

The grids used for all calculations are structured meshes. Fig. 3 shows two typical grids used for aligned and staggered configurations. The light color regions represent solid areas.

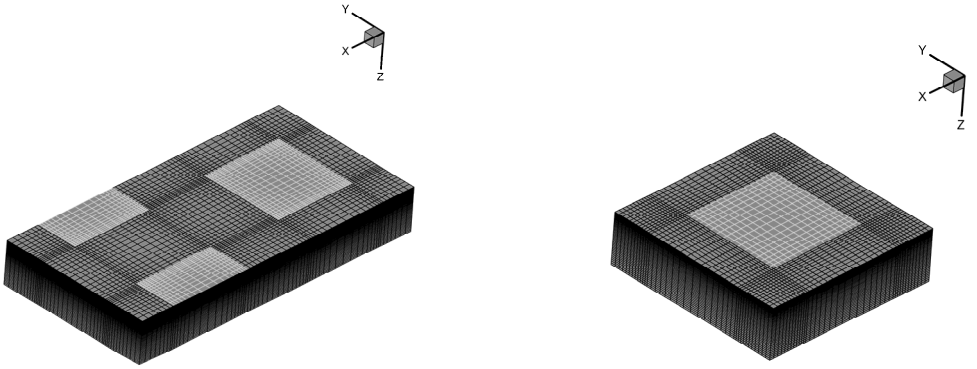


Fig. 3: Two typical grids used for numerical calculations for staggered (left) and aligned (right) configurations.

To study the effect of grid size, the friction factor-Reynolds number product for three different grid sizes are obtained in the case of large velocity gradient. This case is associated with the condition in which $W_m = 0.9$ and $Re = 2000$. Table 1 and 2 present this product at different value of cavity fractions for aligned and staggered microposts. As these tables show, little differences exist between the results of different grid sizes. So, at all values of cavity fraction, the lowest grid size suffices for good prediction of friction factor-Reynolds number products. Since the grid study is performed for the case of large velocity gradient in the channel, thus the lowest grid size corresponds to each cavity fraction is appropriate for numerical computation at the lower values of relative module width and Reynolds number.

Table 1: The friction factor-Reynolds number product for aligned microposts at $W_m = 0.9$ and $Re = 2000$

| | $F_C = 0.1$ | $F_C = 0.3$ | $F_C = 0.5$ | $F_C = 0.7$ | $F_C = 0.9$ | $F_C = 0.97$ |
|---|---|---|---|---|---|---|
| Grid size | 40095 | 35280 | 81000 | 72000 | 54000 | 37845 |
| f . $Re$ | 94.22 | 83.09 | 64.98 | 42.62 | 20.45 | 10.50 |
| Grid size | 67500 | 61250 | 107500 | 96800 | 84640 | 72200 |
| f . $Re$ | 94.30 | 83.53 | 65.01 | 42.75 | 20.51 | 10.58 |
| Grid size | 88985 | 93492 | 140450 | 143312 | 114600 | 107325 |
| f . $Re$ | 94.32 | 83.67 | 64.87 | 42.75 | 20.45 | 10.59 |

Table 2: The friction factor-Reynolds number product for staggered microposts at $W_m = 0.9$ and $Re = 2000$

| | $F_C = 0.1$ | $F_C = 0.3$ | $F_C = 0.5$ | $F_C = 0.7$ | $F_C = 0.9$ | $F_C = 0.97$ |
|---|---|---|---|---|---|---|
| Grid size | 62900 | 78255 | 82600 | 93960 | 53320 | 82305 |
| f . $Re$ | 94.43 | 88.49 | 80.48 | 70.82 | 36.62 | 17.38 |
| Grid size | 104000 | 104550 | 105651 | 129150 | 92510 | 102300 |

| f . $Re$ | 94.47 | 88.48 | 80.49 | 71.97 | 36.47 | 16.60 |
|---|---|---|---|---|---|---|
| Grid size<br>f . $Re$ | 135000<br>94.5 | 130592<br>88.49 | 138600<br>80.77 | 150150<br>71.91 | 126852<br>36.52 | 126140<br>16.62 |

## 4. Results and Discussions

To validate the results, the slip length that is normalized by the distance between two adjacent posts obtained from the present simulation at Reynolds number of $Re = 11.85$ for aligned and staggered microposts is presented in Fig. 4. In this figure, the theoretical [5] and experimental results [17] are also included. As this figure presents, a good agreement exist.

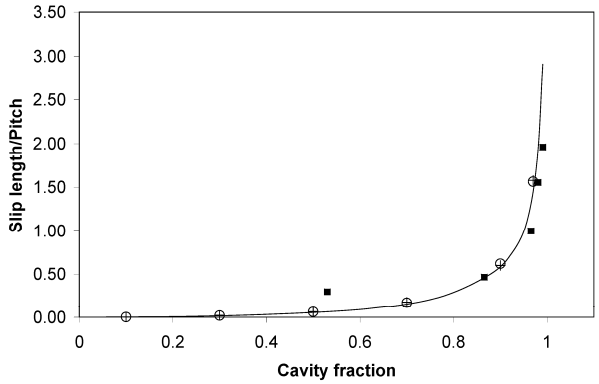


Fig. 4: Normalized slip length for present study and those reported in the literature. Present study (aligned (+) and staggered (O) microposts), theory of Ybert et al. [5] (solid lines) and experimental results [17] (solid square).

Fig. 5 illustrates the line plot of friction factor-Reynolds number product versus cavity fractions. This product is obtained for six different values of cavity fractions, $F_c = 0.1, 0.3, 0.5, 0.7, 0.9$ and $0.97$. In these figures, three different values of relative module width, $W_m = 0.1,\ 0.5$ and $0.9$ are also concerned.

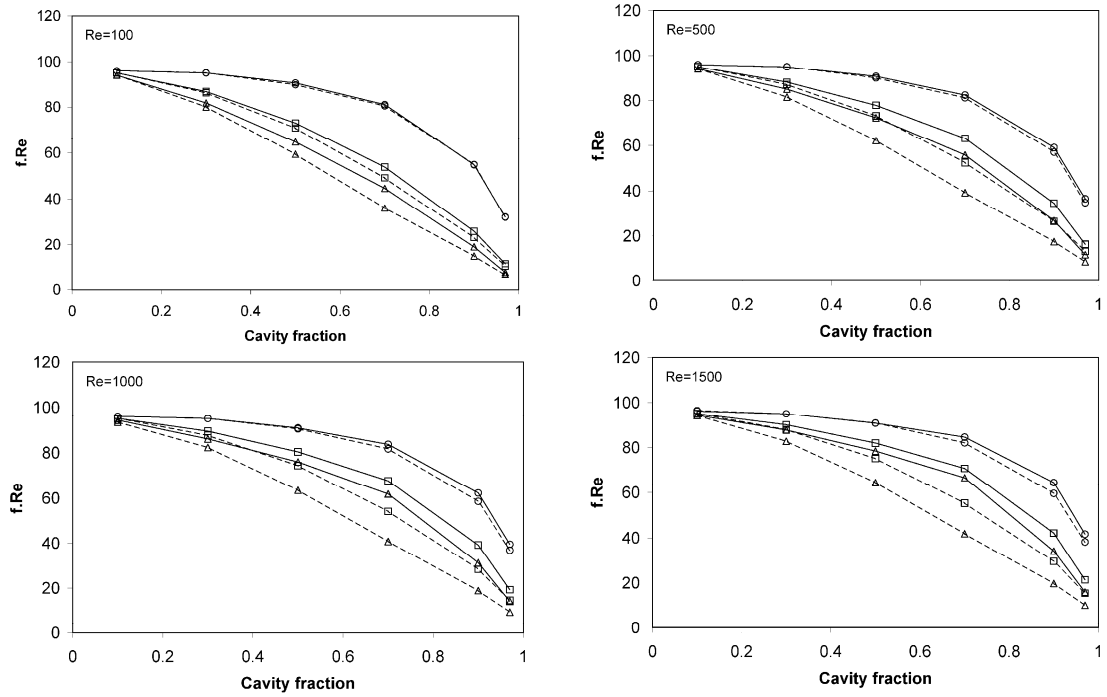

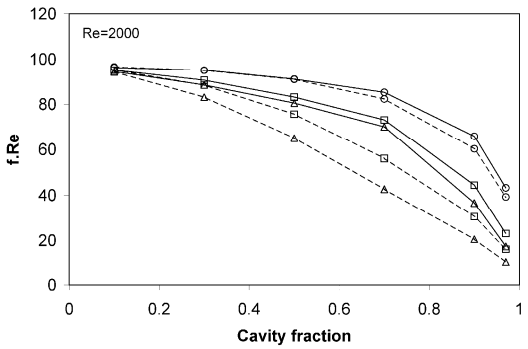


Fig. 5: The friction factor-Reynolds number product versus cavity fractions at different values of relative module width, $W_m = 0.1$ (circle), $W_m = 0.5$ (square) and $W_m = 0.9$ (triangle). Solid and dashed lines are associated with the staggered and aligned configurations, respectively.

As presented in this figure, the friction factor-Reynolds number product for aligned arrangement is lower than that of staggered one. This figure shows that at a fixed Reynolds number, the difference between the friction factor-Reynolds number products for these two arrangements increases with increasing value of relative module width. It can also be seen that at a fixed value of relative module width, the deviation between these two configurations increases with increasing values of Reynolds number.

Fig. 6 depicts the line plot of slip length that is non-dimensionalized by the distance between two adjacent posts versus cavity fraction. The values of cavity fraction and relative module width used for line plot are those presented in Fig. 5. In this figure, two values for Reynolds number (i.e. $Re = 500$ and $1000$) are considered.

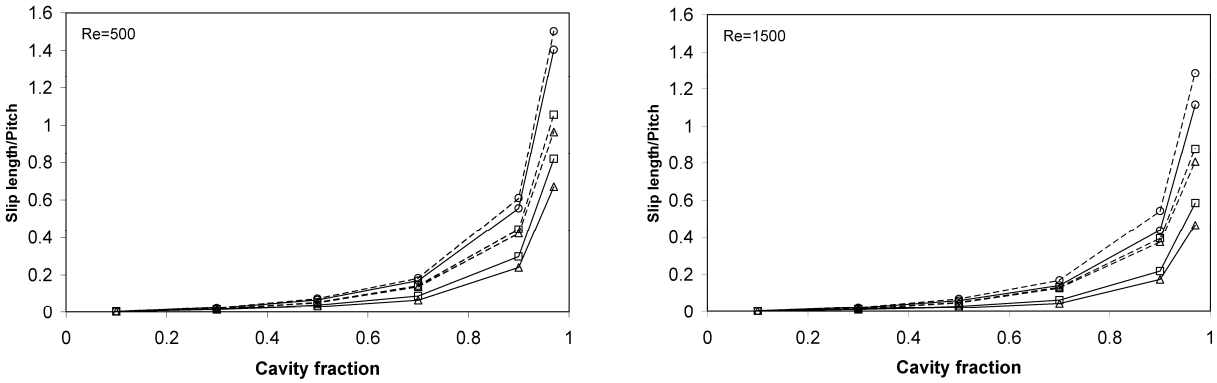


Fig. 6: The non-dimensional slip length versus cavity fractions at different values of relative module width, $W_m = 0.1$ (circle), $W_m = 0.5$ (square) and $W_m = 0.9$ (triangle). Solid and dashed lines are associated with the staggered and aligned configurations, respectively.

The results presented in Fig. 6 show that the non-dimensional slip length for aligned microposts is higher than that of staggered arrangement. This figure presents higher deviation for non-dimensional slip length for increasing values of relative module at a fixed value of Reynolds number.

## 5. Conclusion

In this study, laminar drag reduction through microchannels with superhydrophobic walls consist of aligned and staggered microposts is investigated. Numerical results show that at a same value of Reynolds number and relative module width, the aligned configuration provides less friction factor-Reynolds number product in comparison with staggered posts. The difference in this product between these two configurations increases with increasing values of relative module width. Results show that at a fixed value of relative module width, the deviation in this product increases as the Reynolds number increases. The results also show that the non-dimensional slip

length for aligned configuration is more than that of staggered arrangement and the difference between two configuration increases with increasing values of relative module width.

## 6. References


[1] M. A. Samaha, H. V. Tafreshi, M. Gad-el-Hak. Modeling drag reduction and meniscus stability of superhydrophobic surfaces comprised of random roughness. Phys. Fluids. 2011, 23: 012001.

[2] J. R. Philip. Flows satisfying mixed no-slip and no-shear conditions. Z. Angew. Math. Phys. 1972, 23: 353-72.

[3] J. R. Philip. Integral properties of flows satisfying mixed no-slip and no-shear conditions. Angew. Math. Phys. 1972, 23: 960-68.

[4] C. Cottin-Bizonne, C. Barentin, E. Charlaix, L. Bocquet, J.-L. Barrat. Dynamics of simple liquids at heterogeneous surfaces: molecular dynamics simulations and hydrodynamic description. Eur. Phy. J. E. 2004, 15: 427-38.

[5] C. Ybert, C. Barentin, C. Cottin-Bizonne, P. Joseph, L. Bocquet. Achieving large slip with superhydrophobic surfaces: scaling laws for generic geometries. Phys. Fluids. 2007, 19: 123601.

[6] J . Ou, and J.P. Rothstein. Direct velocity measurements of the flow past drag-reducing ultrahydrophobic surfaces. Phys. Fluids. 2005, 17: 103606.

[7] M. Sbragaglia, R. Benzi, L. Biferale, S. Succi, F. Toschi. Surface roughness-hydrophobicity coupling in microchannel and nanochannel flows. Phys. Rev. Lett. 2006, 97: 204503.

[8] J. Davies, D. Maynes, B. W. Webb, B. Woolford. Laminar flow in a microchannel with superhydrophobic walls exhibiting transverse ribs. Phys. Fluids. 2006, 18: 087110.

[9] D. Maynes, K. Jeffs, B. Woolford, B.W. Webb. Laminar flow in a microchannel with hydrophobic surface patterned microribs oriented parallel to the flow direction. Phys. Fluids. 2007, 19: 093603.

[10] A. Hirsa. Inertial and channel confinement effects on laminra flow in microchannels with superhydrophibic surfaces. 62nd anuual meeting of the APS division of fluid dynamics, Minnesota, Nov. 24-24, 2009.

[11] M. B. Martell, J.B. Perot, J.P. Rothstein. Direct numerical simulations of turbulent flows over superhydrophobic Surfaces. J. Fluid Mech. 2009, 620: 31–41.

[12] K. Jeffs, D. Maynes, B. W. Webb. Prediction of turbulent channel flow with superhydrophobic walls consisting of micro-ribs and cavities oriented parallel to the flow direction. Int. J. Heat & Mass Trans. 2010, 53: 786-796.

[13] J. Ou, J.B. Perot, J.P. Rothstein. Laminar drag reduction in microchannels using ultrahydrophobic surfaces. Phys. Fluids. 2004, 16: 4635–60.

[14] C.-H. Choi, and C.J. Kim. Large slip of aqueous liquid flow over a nanoengineered superhydrophobic surface. Phys. Rev. Lett. 2006, 96: 066001.

[15] R. J. Daniello, N. E. Waterhouse, J. P. Rothstein. Drag reduction in turbulent flows over superhydrophobic surfaces. Phys. Fluids. 2009, 21: 085103.

[16] Y. P. Cheng, C. J. Teo, B. C. khoo. Microchannel flow withsuperhydrophobic surfaces:Effects of Reynolds number and pattern width to channel height ratio. Phys. Fluids. 2009, 21: 122004.

[17] C. Lee, C.-H. Choi, C.-J. Kim. Structured surfaces for giant liquid slip. Phys. Rev. Lett. 2008, 101: 064501.